Structural Characterisation and Docking Studies of Copper Homocysteine Complex with Cytochrome c Oxidase, Glutathione Peroxidase, Superoxide Dismutase for Evaluation of Metal Mediated Homocysteine Toxicity

P. Jhansi Lakshmi[1*]

[1]*Department of chemistry, R.B.V.R.R Women's college, Hyderabad, Narayanaguda, Hyderabad, Telangana, India*

***CORRESPONDING AUTHOR:**

P. Jhansi Lakshmi
Email: jhansipadithem@gmail.com

ISSN : 2382-5359(Online), 1994-1412(Print)

DOI:
https://doi.org/10.3126/njst.v22i2.78605

Date of Submission: 8 Feb, 2023

Date of Acceptance: 2 Jun, 2024

Copyright: The Author(s) 2023. This is an open access article under the CC BY license.

ABSTRACT

An emerging understanding of the role and regulation of homocysteine metal ion interactions during oxidative injury which leads to vascular pathogenesis underlines metal ion importance and need for more research on this aspect. In the present work metal ion interactions in solution and as well as solid state were carried out. Synthesized Cu (II), Ni (II) and Zn (II) complexes with homocysteine. The complexes were further characterized spectrally with IR, UV, Mass, ESR, X-ray photoelectron spectroscopy and TGA techniques. The possible geometries of metal complexes were evaluated using the molecular mechanics calculations. The refined structures were screened based on lowest strain energies calculated by applying MM3 force field. The molecular docking study of copper complex was performed by using Autodock4.2 software against Cytochrome C oxidase, Glutathione peroxidase 1 and Superoxide Dismutase 1 enzymes. Based on analytical, conductance, magnetic and electronic spectral data the Cu (II) and Zn (II) complexes are assigned tetrahedral geometry and Ni (II) complex is assigned square planar geometry. These complexes are formulated as [M(L)H2O]. The formation constants for the interaction of metal ions with homocysteine under physiological conditions as well as the structure and composition of metal complexes synthesized provide some evidence to earlier biochemical studies on animal models. The docking values obtained in the present study may provide supporting information for the biochemical studies related to homocysteine toxicity in presence of metal ions. The binding interactions at these enzymes active site revealed that copper homocysteine complex interaction led to Inhibition of COX, SOD and Glutathione peroxidase enzymes activity, a possible mechanism for therapeutic intervention to treat diseases caused by homocysteine toxicity.

Keywords: Copper homocysteine complex , Cytochrome C oxidase , docking studies, Formation constants, Glutathione peroxidase 1 , Homocysteine toxicity Superoxide Dismutase

1. INTRODUCTION

The transition metal ions inevitably exist as metal complexes in biological systems by interaction with the numerous biomolecules possessing functional groups capable of complexation or chelation G.L. Eichorn (1973), H. Sigel, Marcell Dekker (1998), M. N. Hughes (1981). In all metallobiomolecules the essential metal ions such as Cu, Zn, Cr, Fe, Mn, and Co exist as binary, and ternary chelates of amino acids, carboxylic acids and proteins. Without these interactions, life could not exist or even come into being without the mediating action of metal ions. This is evident by the role of metal ions in many biological processes such as: catalytic activity of metalloenzymes, regulation of nucleic acids replication, pharmacological activity of many metal complexes, etc. Bertini, I.; Gray, H.B (2007), Ferré-D'Amaré AR, Winkler WC. (2011), Kaluđerović GN, et al. (2012), Katherine J. Franz and Nils Metzler-Nolte (2019). In all metalloenzymes the metal ion is usually coordinated with nitrogen, oxygen or sulfur atoms belonging to amino acids in the polypeptide chain incorporated into the protein.

The interactions between the amino acid and the metal ions are thus considered as models of the processes which take place at the molecular level in the metal protein system. Although studies of the systems of metals with various amino acids have been carried out (Farkas, E. & Sovago, I., 2007; Z. Ozturk et al. 2014; Ahmed, Mahmood & Qadir, Muhammad. 2014; Arunadevi, Alagarraj, and Natarajan Raman (2020) detailed information on the mode of coordination of homocysteine (hCy) with metal ions at biological conditions in solution are not available. In order to get a better understanding of the toxic effects of homocysteine, studies are carried out in solution and solid state of various metal ion interactions with homocysteine at physiological conditions ($t=37^0$, $\mu=0.15M$). The homocysteine molecule is potentially a tridentate ligand and may chelate with the metallic cations using the carboxylate oxygen, amino nitrogen, and thiolate sulphur as the donor atoms. In the blood, homocysteine being very active can form binary complexes, the physiological action of homocysteine is connected with its ability to form complexes with metal ions (Dong D et al. 2013; Keskitalo, Salla et al. 2014; Ledda C et al. 2019) including Cu^{2+}, Zn^{2+}, Ni^{2+}, Co^{2+}, Cd^{2+} and Pb^{2+}. Determining the stability of the metal complexes and their structures will be helpful in understanding the physiological function of this amino acid . In the present study, copper homocysteine complex synthesized was docked with COX1, SOD1 and Glutathione peroxidase enzymes to understand the copper mediated catalytic activity of these enzymes and to provide possible mechanism for copper mediated homocysteine toxicity (Hultberg et al. 1997; Fan, X et al. 2020).

2. MATERIALS AND METHODS

2.1 pH METRIC STUDIES

Evaluation of formation constants for binary metal complexes ML containing hCy with transition metal ions like Cu (II) Co(II), Ni(II), Zn(II), Cd(II) and Pb(II) were studied potentiometrically. Further detailed physico chemical studies of the mixed ligand complexes (ML_nA_n ; where n=1) containing the following L and A ligands has been carried out. Ligand L : Homocysteine (primary ligand) **:** Ligands A (Secondary ligands) : $N\text{-}O^-$ donors: α –alanine, β- alanine, N-N donors: 2,2' –bipyridyl, 1,10-phenanthroline $^-O\text{-}O^-$donors: Oxalic acid, malonic acid, pyrocatechol. The formation constants are evaluated at the physiologically relevant temperature (37.0 ^{0}C) and ionic strength (μ = 0.15M) by a pH – metric method involving the titration of solutions containing 1:1 molar ratio of metal ion and ligands L for binary systems with standard carbonate free sodium hydroxide. In the present investigation the computer program "Stability constants of Generalized Species" [SCOGS] Sayce IG (1968) was used to calculate the protonation constants of the free ligands and formation constants of the protonated, mono binary, bis binary metal complexes. SCOGS can be used to analyze appropriate pH titration data to yield protonation constants, metal ion hydrolysis constants, stability constants of simple complexes (ML, ML_2, etc.), stability constants of polynuclear species (M_2L_3 , M_2L_4 , M_2L_2OH etc.) . In addition to this, distributions and concentrations of various species present as a function of pH were also computed from known constants and are presented in the form of pH species distribution profiles by using the computer programme SPE (Smith, Robert M et al. (1985), Rajarajan, Govindasamy et al. 2021) such profiles are very useful in visualizing the nature and concentrations of various species present in solution, under a given set of conditions.

2.2 Synthesis, Spectral Characterisation Of Homocysteine Binary Metal Complexes

In the present work we have synthesized the complexes of homocysteine with Cu(II), Ni(II) and Zn(II) and had attempted to understand the mechanism of copper mediated homocysteine induced vascular pathogenesis and Alzheimer's disease. In blood, homocysteine molecules possess the ability to form chelate complexes with metallic cations through coordinate covalent bonds with the negatively charged carboxylate oxygen, the amino group nitrogen and the thiolate group sulphur.

2.2.1 Synthesis of Cu(II) & Ni(II) homocysteine complexes:

The Cu(II) complex was obtained as follows: 0.0676g hCy (Sigma-Aldrich) in 5ml aqueous Cu(II) solution containing 0.0852 g $CuCl_2.2H_2O$ at a 1:1 molar ratio Cu:hCys. This resulted in formation of a solid blue Cu (II) complex, that precipitated after 24 hrs. The crystalline powder was filtered and collected under vacuum. The Ni(II) complex was obtained as follows: 0.0676g hCy (Sigma-Aldrich) in 5ml aqueous Ni(II) solution containing 0.0952 g $NiNO_3$ at a 1:1 molar ratio Ni:hCy. This resulted in formation of a brown solid complex that precipitated after 24 hrs.

2.2.2 Ir And Esr Studies

Infrared spectra were obtained on a FTIR instrument in the range of 4000- 400cm^{-1}. The electronic paramagnetic resonance spectra (EPR) of the copper complex were recorded on Varian-E-112 at room temperature.

2.2.3 X-Ray Photoelectron Spectral Studies (Xps)

The XPS spectra are recorded on a VG Escalab 200 MK spectrometer equipped with an Al-Kα source and a hemispherical analyzer connected to a five-channel detector. The spectra are recorded with constant pass energy of 20 eV. Binding energies were determined by computer fitting of the measured spectra . Powder samples are mounted for analysis. The most widely used method is dusting the powder onto a polymer-based adhesive tape with a camel-hair brush.

2.2.4 Mass Spectra

The EI mass spectra were recorded on a VG micromass 7070-H instrument, ESIMS spectra were recorded on VG AUTOSPEC mass spectrometer.

2.2.5 Electronic Spectra

Electronic spectra of metal complexes in DMSO were recorded on Schimadzu UV-VIS 1601 spectrophotometer.

2.2.6 Magnetic studies

Magnetic susceptibilities of the complexes were determined on Gouy balance model 7550 using Hg [Co $(NCS)_4$] as standard. The diamagnetic corrections of the complexes were computed using Pascals constants.

2.2.7 Thermal studies

TGA of metal complexes were carried on Mettler Toledo Star system in the temperature range of 0-1000^0 C.

3. MOLECULAR MECHANICS AND DOCKING STUDIES OF HOMOCYSTEINE BINARY METAL COMPLEXES

The possible geometries of metal complexes were evaluated using the Molecular mechanics calculations with Hyperchem and Mopac packages. Initially the atomic charges of each complex were calculated by a semi-empirical method (ZNDO). The structures using the standard force field included in the package, further refinement was done for the complexes . The refined structures were screened on the basis of the lowest strain energies. The energies of the resulting systems were calculated using the MM3 forcefield. Copper homocysteine metal complex docking studies were carried out into Cytochrome C oxidase1, Glutathione peroxidase 1 and Superoxide Dismutase 1 enzymes (Zong, S et al. 2018; Manjula, R et al. 2018) using Autodock4.2 software (Morris GM, 2009). Docking of Copper homocysteine metal complex was carried out on crystal structures of Cytochrome C oxidase (PDB_ ID: 5Z62), Glutathione peroxidase 1(PDB_ID: 2F8A), and Superoxide Dismutase 1 (PDB_ID: 5YTO). These PDB structures were retrieved from protein data bank. During the docking for Cytochrome C oxidase we have used 0.375Å grid box parameters as centre: x = 326.731, y = 340.743, z = 247.895 and grid box size: x=40, y=42, z=40. For Glutathione peroxidase 1 we have used 0.375Å grid box parameters as centre: x = -0.939, y = 22.701, z = 27.518 and grid box size: x=42, y=42, z=52 and for Superoxide Dismutase 1 we have used 0.375Å grid box parameters as centre: x = 51.881, y = 62.96, z = -17.525 and grid box size:

x=40, y=42, z=48. While docking 10 conformations were generated for each ligand by using default genetic algorithm. In this study, input preparation carried out using MGLtools-1.5.6 and final docking performed in Autodock 4.2. The interaction of the metal complexes with DNA was also studied by molecular modelling with special reference to docking.

4. RESULTS AND DISCUSSION

4.1 Acid Dissociation Constants For Free Ligand (L)

The pH titration curve shown in **Fig-1** was obtained by adding increasing amounts of alkali to free ligand containing hCys in (H_3L) form. The pH titration curve in the presence of three protons shows a steep inflection at a=1(a= moles of base added per mole of ligand) followed by a buffer region ending a=3 with a small inflection at a=2. The titration curve at low pH region showed the dissociation of –COOH group and at high pH the simultaneous dissociation of $–NH_3^+$ and –SH groups was observed. From the potentiometric titration data for the ligand hCys the dissociation constants were computed from the computer programme SCOGS by taking into consideration the relevant species H^+, H_3L, H_2L, HL and L. The dissociation constants thus obtained for hCy at 37^0 C and μ = 0.15M (KNO_3) ionic strength were listed in **Table-1** and a schematic representation of the ligand dissociation is given in **Fig-2.** The pK_{1a} value is assigned to dissociation of a proton from the carboxylate oxygen. The pK_{2a} and pK_{3a} values are in very close proximity and hence the dissociation of both the amino and thiol protons may be taking place simultaneously in the buffer region of a=1 to a=3. A pH ligand species profile for hCys is represented graphically in **Fig-3**. The maximum concentrations of the various species and the corresponding pH values are H_2L =90.91% at pH=2.0, HL = 98.24% at pH 7.0 and L=99.30% at pH=12.

4.2 Binary Metal Complxes Of Homocysteine (L)

The formation constants of metal complexes formed by interaction of M(II) {Cu(II), Ni(II), Ca(II), Mg(II), Pb(II), Cd(II), Co(II) and Zn(II)} with hCy were studied. The potentiometric titration curves for the interaction of various metal ions with homocysteine in presence of three moles of acid taken in a 1:1 molar ratio are shown in **Fig-4**. For binary systems involving the metal ion Cd (II) hydrolysis and precipitation was observed from the beginning of the titration. For Ca (II) and Mg(II) , the free ligand curve and the metal ligand curve overlapped with each other over the entire pH range, indicating lack of metal complex formation. The formation constants for the binary metal complexes were calculated from the potentiometric data with the computer programme SCOGS by taking into consideration the species H_3L, H_2L, HL, L, and ML. The formation constants for the following equilibrium $M + L \leftrightarrow ML$

are listed in **Table-2**. From data in **Table-2** order of stability of metal complexes is Cu(II)>Pb(II)>Ni(II)>Zn(II)>Co(II). Cu (II) complexes are more stable because of Jahn Teller distortion of the metal ion which provide strong four equatorial sites and weak two axial sites. The Pb (II) complexes are considerably stable because of the high affinity between the soft 'S' donor site on the ligand and soft Pb (II) metal.

All the complexes are stable at room temperature and are non hygroscopic. On heating they decompose without melting. The complexes are insoluble in water and are soluble in DMSO and DMF.

Elemental Analysis: The analytical data of the complexes are presented in **Table-3**. It is clear from the table that the theoretical values calculated for the composition shown for each of the complexes are in good agreement with the experimental values. The composition assigned to the complexes may therefore be justified.

4.3 IR Data

The spectra of metal complexes were compared with spectra of pure ligand hCys (B.B Ivanova et al. 2004). Homocysteine showed absorption bands in the range 2300-2800cm^{-1} corresponding to $\nu(NH_3^+)$, a band at 2610cm^{-1} assigned to ν (SH) and two bands at 1680+1620 cm^{-1} ,corresponding to $\delta(NH_2)+ \nu(COO^-)$. The stretching frequencies were compared and illustrated in the **Table-4** for various metal ions. The IR data for the blue copper complex **Fig-5** was compared with free homocysteine spectra. The complexation with Cu (II) ions led to disappearance of the band in the 2300-2800cm^{-1} due to NH_3^+ deprotonation and NH_2 coordination to Cu(II). Coordination to the NH_2 and COO^- groups followed from shift of the bands at 1680 and 1620 cm^{-1} to 1640 and 1610cm^{-1}. The complexation with SH group was observed from the disappearance of

the 2610 cm^{-1} band. The bands ν(Cu-S) at 646cm^{-1} , ν(Cu-N) at 561cm^{-1}, showed the metal coordination in blue complex. ν(Cu-O) bands usually were observed around 340cm^{-1} which we could not record with our instrument. The spectra recorded for nickel complex showed **Fig-6** major absorption bands in the range 1342-1095cm^{-1} corresponding to ν(C-O),a band at 2610cm^{-1} was missing assigned to ν(S-H), predicting the possibility for thiol group coordination with Ni, which is evident for the presence of band ν(Ni-S) at 648cm^{-1} .The decrease in stretching frequency of carbonyl group observed at 1653 cm^{-1} in free hCys to 1575 cm^{-1} in the complex shows that COO^- is coordinated with Ni. The band ν (Ni-N) at 536 cm^{-1}, showed the metal coordination with $–NH_2$ group. In accordance with the literature data these facts indicate a tridentate coordination of hCys to metal Ions. The IR data for the complex [Ni(hCy) (H_2O)] was compared with other spectral techniques (Kazuo Nakamoto ,1978),

4.4 Esr & Mass Spectral Data

The room temperature ESR spectra of blue copper complex in methanol solution showed a single signal **Fig-7**. The three g_x= 2.072, g_y= 2.126, and g_z= 2.188 are similar and show the presence of Cu(II) in an isotropic environment. ESR spectra for the Cu(II) complex could not be obtained at lower temperatures. Further, we were not able to obtain monocrystals of proper size for X-Ray investigation. The EI spectra of [Cu(hCy)(H_2O)] **Fig-8** exhibits molecular ion peak for the mononuclear complex [Cu(hCy)(H_2O)] at m/z=218. (M+He), peaks at m/z=222 is due to Sulphur isotopes

4.5 Electronic spectra

The electronic spectra of [Cu(hCy)(H_2O)] and [Ni(hCy) (H_2O)] are shown in **Fig-9,10**. [Cu(hCy)(H_2O)] showed three peaks around 15,500; 17,710 and 22,200 cm-1 **Table-5** that have been assigned respectively to the transitions $^2B_{1g} \rightarrow {}^2A_{1g}$; $^2B_{1g} \rightarrow {}^2A_{1g}$ and $^2B_{1g} \rightarrow {}^2E_g$ (S. N. Bolotin et al. 2009). The Ni(II) complex of hCy showed two peaks one at 18,900 and the other at 27,350 cm-1. The complex was found to be diamagnetic (Vijayalakshmi M. / IJPS 2019; 15 (3):29-40). Further, it is reported that the diamagnetic square planar Ni(II) complexes do show an absorption band of medium intensity in the region 16,662 - 22,220 cm-1. In view of these observations the peak appearing around 18,900 cm-1 in the present complex has been assigned to $^1A_{1g} \rightarrow {}^1A_{2g}$. One of the transitions proposed for square planar Ni(II) complex(W. Roy Mason, and Harry B. Gray (1968) and the other peak appears at 27,350 cm-1 may be due to charge transfer. The three transitions obtained for [Cu(hCy)(H_2O)] and two transitions for [Ni(hCy)(H_2O)] are compatible with tetrahedral and square planar geometries.

4.6 X-Ray Photoelectron Spectral Data

4.6.1 XPS DATA of Cu(II) complex: The whole spectrum of the complex recorded **Fig-11(a-f)** and list of binding energies are given in **Table-6** showed the photoelectron lines for Cu ($2p_{3/2}$ and $2p_{1/2}$), C (1s), O (1s), N (1s), and S (2p). The binding energy values of Cu $2p_{3/2}$ observed at 934.6eV and 953eV, predicts copper in Cu(II) state, the higher in shift compared to the literature data is due to oxygen environment and the Cu-O bond present in the complex which is stronger increasing the Cu binding energy values. Two peaks for O1s B.E are observed at 531.925eV and 533.801eV. The more intense peak at 531.925eV can be correlated with oxygen B.E in a metal environment.. This is in agreement with Cu peaks observed at 934.6eV. Thus the B.E values for Cu are effected by O environment. The O 1s peak at 533.801eV correlates with literature data of O in H_2O molecule. The three main peaks of 1s of C are observed at a binding energy values of 284.638 eV, 286.706 eV and another one around 289.130 eV. The B.E 284.638 eV is due to C-C bond, the B.E 286.706 eV is due to C-S bond and the peak at 289.130 eV is due to C-N bond present in the complex. The peak for carbonate moiety is less intense and the difference in B.E values for C-N and -CO_2 being less are obtained as broad peak in the overall spectrum recorded for C in the complex. The main peak of 2p of S is observed at 168.517ev. The shift in value of 3 eV is compared with respect to sulphur B.E value 165.110eV of free Cysteinemonohydrochloride compound. The increase in binding energy value can be attributed to Cu coordination with sulphur of homocysteine and thus Cu-S bond formation can be predicted in the complex of [Cu(hCy)(H_2O) complex. The B.E value of N 1s in free cysteinemonohydrochloride is observed at 401 eV, the similar peak in Cu-hCy complex is observed at 399.946 eV, the shift of ~1.0 eV to the lower side can be explained due to decrease in electron density on nitrogen atom and this decrease can be explained due to formation of coordinate bond between Cu and N in formation of Cu-hCy complex. (Appendix)

4.6.2 XPS DATA OF Ni(II) complex: Surface characterization of [Ni(hCy)(H_2O) complex recorded obtained the photoelectron lines as shown in **Fig-12a-f**

for Ni ($2p_{3/2}$ and $2p_{5/2}$), C (1s), O (1s), N (1s), and S (2p). The two major peaks at 855.901 eV and 873.443 eV are identified for Ni atom B.E. The correlation table for Ni B.E values listed in the Appendix had one line at 855.1 eV for Ni-S environment which is in accordance with 855.901eV observed for the complex recorded. The peaks for C 1s based on the literature available are assigned as 1s B.E 284.582 eV for C-C bond, 1s B.E 287.281 eV for C-S bond, 1s B.E 289.271 eV for C-N bond and a small intense peak of 1s B.E 291.282 eV for carbonate anion. The peak for carbonate anion is more evident in this complex when compared to copper complex showing slight difference in the environment of carboxylate anion in the copper complex to the nickel compound. The B.E energy value is at higher side because of possibility of hydrogen bonding with aquo group attached to Ni and carboxylate oxygen of hCy moiety bonded with Ni with tridentate manner as shown in molecular modelling generated structure of Nickel complex. The tridentate geometry is further confirmed by the peaks observed for N1s at 402eV due to Ni-N bond formation and S2p B.E at 165.110eV due to Ni-S bond formation. The B.E values for S 2p and N1s are compared with cysteine monohydrochloride, expected to present at 163.1eV(S 2s) and 401 eV (N 1s). The major shift in the above B.E values from expected shows the possibility of coordination with metal atom. The B.E of free S in cysteinemonohydrochloride is less. But when sulphur is bound to Nickel ion a strong bond is formed which is evident by high B.E of 165.110eV. The same can be explained with N 1s B.E value. The major peaks in overall spectrum of nickel complex thus showed peaks for Ni-O, Ni-N, Ni-S and Ni-OH_2. (Appendix)

4.7 Thermogravimetric data :

TGA of metal chelates are used to get information about the thermal stability of complexes and decide whether the water molecules (if present) are inside or outside the coordination sphere. Lattice water is lost at lower temperature regions between 60-100^{o}C whereas the loss of coordinated water requires temperature above 100^{o}C. In other words, depending upon the value of the temperature at which water is lost, it can be identified as one of these two kinds i.e. lattice or coordinated water. TGA involves a change in the weight of a compound with an increase in temperature and the data is represented in the form of thermogram which is a plot of weight Vs temperature. DTA involves the measurement of a change in heat content as a function of difference in temperature between the sample and reference compound. The DTA data is represented in the form of endothermic/exothermic peaks. In the present investigation heating rates were suitably controlled at 10 ^{o}C min^{-1} under nitrogen atmosphere, and the weight loss was measured from the ambient temperature upto 1000^{o}C. The TGA curves of [Cu(hCys)(H_2O)] show that the initial mass loss occurring within 100-120^{o}C range is interpreted as loss of one coordinated water molecule. The thermo gram above this temperature (>500 ^{0}C) is horizontal and the final product of decomposition at this temperature region corresponds to their metal oxides (] S. Chandralekha et al. 2014). The Thermogram of [Cu(hCys)(H_2O)] is given in **Fig-13.** Presence of water molecule is further confirmed by the endothermic bands observed in the respective DTA curve in the temperature region where the TGA curves showed loss in weight. In addition to the endothermic bands, the DTA curves of complex also show exothermic bands. These bands appeared at higher temperatures which represent phase transition, oxidation and/or decomposition of the compound. López-Gastélum, K. et al. **2021**.

4.8 Molecular Modelling studies

Metal complexes will adopt the geometry which is having the least energy. Hence Molecular Mechanics calculations were calculated for various possible geometries for the metal complex of homocysteine with a given metal ion. The optimization of geometry and energy values were calculated by molecular mechanics software (System Type- Molecular Mechanical Hamiltonian UFF). For Cu (II) distorted octahedral, square planar or tetrahedral geometry are possible, however Molecular Mechanics calculations showed that for homocysteine Cu (II) complexes tetrahedral geometry is having the least energy **Fig-14**. For Ni (II) octahedral, square planar or tetrahedral geometry are possible. However, the modeling calculations showed that homocysteine complex with nickel showed a square planar geometry which has the lowest energy state **Fig-15**

4.8.1 Molecular docking studies Analysis- Docking interactions of (Cu(hCys)(H_2O) with Cytochrome C oxidase 1 enzyme

Investigations of homocysteine neurotoxicity in rat dopaminergic pheochromocytoma cells, human neuroblastoma cells and primary rat cerebellar granule neurons (Linnebank M et al. 2006) revealed binding of copper to homocysteine for COX deficiency. In

the present work ,the binding affinity of Copper homocysteine metal complex with COX enzyme surrounded by the protein residues were analysed using molecular docking studies. The binding affinity of the copper homocysteine metal complex showed good interaction energies with the proteins active sites and the results were shown in the **Table-7**. The structure of the Copper homocysteine metal complex docked in the active site of Cytochrome C oxidase (PDB_ ID: 5Z62) has been consider for the docking analysis **Fig16a,b**. The Copper homocysteine metal complex is stabilized by hydrophobic and Pi-sigma interactions. The homocysteine molecule is showing alkyl and Pi-alky interactions with Val-373, Leu-358 and His-291 residues respectively. The His-291 residue forms a hydrogen bonding interaction with oxygen atom. The sulphur atom formed Pi-sulphur interaction with His-290 residue. It also shows hydrophobic interaction with Asp-364 residue in the active site. The Cu(2+) chelating action of homocysteine and impairement of COX activity represent novel mechanisms of HCys neurotoxicity is evident from our strong binding values obtained by docking studies supports earlier observations (Xiao, Zuo & Dong et al. 2013). The higher stability constant ($logK_{ML}^{M}$= 15.13) from solution studies shows that copper complexes are more stable with hCy when compared to other similar amino acids The synthesis of copper complexes and spectral studies in present work provided the geometry and chemical structure of Cu(II)& Ni(II) complexes. These studies throw an insight into the active site of metalloenzymes involved in pathological action of oxidative stress mediated by Cu(II). Based on the formation constant data and spectral characterization of copper complexes we propose the possible explanation for hCy induced Alzheimer's disease in **Fig-17**. When copper hCy complex is formed it leads to deactivation of COX enzyme and thus the membrane potential of mitochondria is lost leading to mitochondrial dysfunction and immediate release of cytochrome c from mitochondria, which then triggers the apoptotic pathway Michael etal (2006). In this process Caspase-3 protein is excessively activated and thus leads to DNA fragmentation and cell death. If this process takes place in neurons it leads to Alzheimer's disease. Thus based on the above hypothesis we propose that hCy induces apoptosis by COX inactivation followed by excess activation of Caspase-3 protein and neuronal cell death.

4.8.2 Docking interactions of (Cu(hCys)(H_2O) with Glutathione peroxidase 1

Copper homocysteine complex docked in the active site of Glutathione peroxidase 1 (PDB_ID: 2F8A) . The Copper complex is stabilized by hydrogen bonding, hydrophobic and Pi-sulphur interactions **Fig18a&b**. Homocysteine molecule showed Pi-sulphur interactions with Trp-160 residue. The Arg-179, Arg-180 and Gly-48 residues showed hydrogen bonding interactions with homocysteine molecule. Docking values showed interaction of metal complex with Glutathione Peroxidase 1 enzyme. Our results support that Cu-hCys complexes affect the metabolism of extracellular thiols more than homocysteine alone and inhibited glutathione peroxidase-1 activity and mRNA abundance made (Apostolova MD et al. 2003).

4.8.3 Docking interactions of (Cu(hCys)(H_2O) with SOD1

The primary form of superoxide dismutase is Cu,Zn superoxide dismutase, which is referred to as SOD1. SOD1 is primarily found in the cytoplasm of cells but a small portion is found in the intermembrane space of the mitochondria. A key feature of SOD1 is that it possesses a copper cofactor, which is used to catalyze the superoxide dismutation reaction. The SOD1 protein is a dimer composed of two identical subunits ,these two subunits are oriented so the two active sites are facing away from each other. Each subunit is composed of 151 amino acid residues. These amino acids are arranged in eight β-sheets and three exterior loops. Each subunit contains a copper ion and a zinc ion at the active site. The copper ion acts as an electron transfer center in this catalyst, while the zinc ion serves as a structural scaffold and a contributes to the positive charge of the active site, which attracts the negatively charged superoxide anion. The placement of the active site of this complex as well as the geometry surrounding the copper metal centers are critical for this reaction to occur. The active site of this complex is at the bottom of a channel. The copper ion is exposed at the bottom of this channel to allow binding of superoxide to the copper ion, while the zinc ion is buried within the protein. This funnel shape leading to the active site is very important to the superoxide dismutase function. Superoxide dismutase has a very small active site compared to the entire size of the enzyme. The small funnel shape is selective towards small molecules such as superoxide. In the funnel shaped channel are copper and zinc cations as well as two positively charged hydrophilic amino acids, histidine and arginine. The strong positive charge provided by these amino acids and metal ions attracts

the negatively charged superoxide to the active site where the superoxide can be converted into less toxic substances. (Bakavayev, S et al. (2019); S. Dayal G et al.(2017).

The structure of the Copper homocysteine metal complex docked in the active site of Superoxide Dismutase 1 (PDB_ID: 5YTO) has been consider for the docking analysis.As in Fig19a&b docking interactions show that the Copper homocysteine metal complex is stabilized by hydrogen bonding, hydrophobic and Pi-alkyl interactions. The homocysteine molecule is showing alkyl interaction with His-80 residue. The His-63, Lys-136 residues formed hydrogen bonding interactions with oxygen atoms. The sulphur atom formed interaction with Lys-136 residue. This complex also shows hydrophobic interaction with Asn-65 residue in the active site. From dock results it is clearly evident that copper complex with homocysteine effectively inhibiting the enzyme activity of above enzymes, due to higher levels of homocysteine in blood causing copper to bind with homocysteine at the active site of enzymes leading to inhibition of SOD1& Glutathione peroxidase enzyme activity, increasing homocysteine toxicity by initiating free radical formation Starkebaum G, et al., (1986) and M.C. Mele and E. Meucci (1996).

4.8.4 Docking interactions at DNA

The docking calculations observed that free homocysteine with DNA got less binding score value (5.13) compared to copper homocysteine with higher dock score=(6.13). Homocysteine and its copper complex can bind to DNA via non covalent interactions by intercalative binding ,groove binding or external electrostatic binding. Among these interactions we observed intercalation mode of binding to DNA with homocysteine and as well as copper homocysteine complex **Fig20a&b** Molecular docking results suggested that the interaction between DNA and Copper homocysteine complex is more stable leading to cellular degradation, the DNA binding values may further give supporting evidence for cytotoxicity of homocysteine (Catalina Carrasco Pozo et al. 2006).

5. CONCLUSION

The potentiometric data determined can be useful in understanding the chelating ability of homocysteine with various metal ions. Cu(II)&Ni(II) complexes of homocysteine have been structurally characterized by different physico-chemical techniques. The metal: ligand stoichiometry in all the complexes was found to be 1:1. All complexes of homocysteine are being associated with one water molecule. The complexes are non-electrolytes in DMF. The coordinating behavior of the ligand homocysteine towards the metals was binegative, tridentate, coordinating thorough oxygen of carboxyl group, nitrogen of amino group and sulfur of thiol group. Ni (II) complex of homocysteine is diamagnetic while Cu(II) complex of homocysteine is paramagnetic to the extent of one unpaired electron. The electronic spectral information of Ni(II) exhibits square planar and the Cu(II) complex tetrahedral in geometry. The higher stability constant ($\log K_{ML}^{M}$= 15) of binary copper –homocysteine complex, shows that copper complexes are more stable with homocysteine when compared to other similar biomolecules like cysteine and penicillamine. The formation constant data and spectral characterization of metal complexes throw an insight into the active site of metalloenzymes involved in pathological action of oxidative stress mediated by Cu(II), due to strong chelating ability of copper with homocysteine and inhibiting enzyme activity of SOD1, COX1 and Glutathione peroxidase enzymes. Docking studies support the physiological action of copper mediated homocysteine toxicity leading to unprogrammed cell death i.e., apoptosis and neuronal cell damage. The redox behavior of homocysteine in presence of copper results in oxidative stress leading to cell death.

ACKNOWLEDGEMENTS

I am grateful to the assistance of IICT, Hyderabad. Thanks for technical support for providing spectral data using Mass, TGA and XPES.

Table 1: Dissociation constants of ligand (l) and secondary ligands(a), temp=37.0° c ; μ=0.15 m kno_3

Ligand L or A	pKa	pK2a	pK3a
DL-Homocysteine(O,S,N)	3.63	8.75	9.67
α- Alanine(N,O)	2.38	9.26	--
2-2'-Bipyridyl(N,N)	1.52	5.88	--
1-10 phenanthroline(N,N)	C.D	4.87	--
Oxalic acid(O,O)	C.D	3.74	--
Malonic acid(O,O)	2.67	5.22	--
Pyrochatechol(O,O)	8.96	11.36	--

*** Constants accurate upto ± 0.02 C.D - Completely Dissociated**

Table 2: Formation Constants For Binary Metal Complexes With Ligand (L)-Homocysteine , Temp=37.0o C ; M=0.15 M Kno3

Metal Ion	logKMML
Cu(II)	15.13
Ni(II)	9.17
Zn(II)	8.72
Pb(II)	10.07
Cd(II)	----
Co(II)	6.42

Constants accurate upto ± 0.02

Table 3: Analytical Data Of The Ligand (Hcy) And Metal Complexes

Compound	M.wt	Colour	C Calc	C Exptl	H Calc	H Exptl	N Calc	N Exptl	M Calc	M Exptl
Homocysteine(hCy)	135.19	White	35.54	35.51	6.71	6.69	10.36	10.38	-----	
[Cu(hCy)(H_2O)]	217.76	Blue	22.06	22.05	5.55	5.53	6.43	6.45	29.18	29.15
[Ni(hCy)(H_2O)]	212.92	Brown	22.56	22.55	5.68	5.66	6.58	6.60	27.57	27.55

Calc- Calculated , Exptl- Experimental

Table 4: The Major Bands Assignments Of Ir Spectra Of Dl-Homocysteine And Its Metal Complexes (Cm-1)

	ν (N-H)	ν (S-H)	ν(-CH_2-)	ν (C-S)	ν (C-O)	ν (C=O)	ν (M-S)	ν (M-N)
hCy	3147	2610	2930	744	1325-1250	1653	------	-------
Cu+hCy (Blue)	3244	-----	916	808	1332-1109	1614	646	561
Ni+hCy (Brown	**3**317	-------	2920	800	1342-1095	1575	648	536
Zn+hCy (White)	3275	-------	2916	900	1338-1114	1577	650	569

Table 5: Electronic Spectral Data Of Complexes

Compound	Frequency (cm^{-1})	μeff B.M
[Cu(hCy)(H_2O)]	15,500(v_1); 17,710(v_2); 22,200(v_3)	1.81
[Ni(hCy)(H_2O)]	18,900(v_1); 27,350(v_2)	-----

Table 6: The Binding Energy Values Of Dl-Homocysteine And The Metal Complexes Of Homocysteine (Ev)

	S 2SeV	O1SeV	C1SeV	N1SeV	Cu 2P3/2,2P5/2eV	Ni 2P3/2,2P5/2eV
hCy	163.2 163.1				------	------
Cu+hCy (Blue)	168.517	531.925 533.801	284.638 286.706 289.130	399.946	934.665 954.387	------
Ni+hCy (Brown	165.110	530.076 532.128 533.351	284.582 287.281 289.279 291.282	402.000	------	855.901 873.443

Table 7:_ Docking Results Of Copperhomocysteine Complex At The Enzyme Sites

S.no.	Protein name	Docking score (in kcal/mol)
1	Cytochrome C oxidase	-4.55
2	Glutathione peroxidase 1	-3.10
3	Superoxide Dismutase 1	-3.62

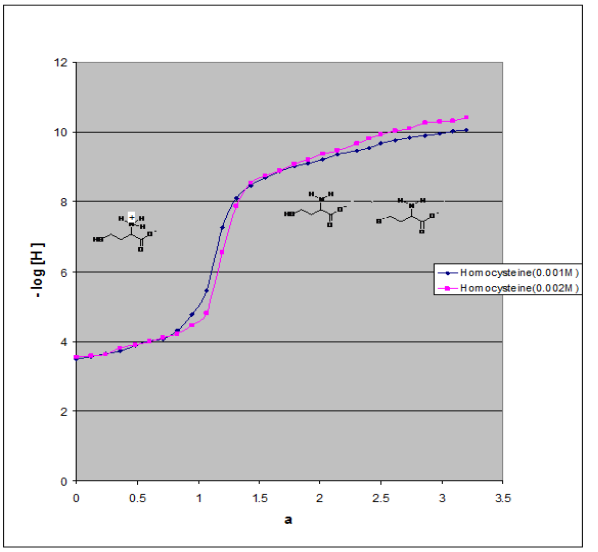

Fig .1: Potentiometric Titration Curve For Free Homocysteine TL = 0.001M; T= 370 C; μ = 0.15 mol dm-3 (KNO3), a = moles of base added per mole of the ligand.

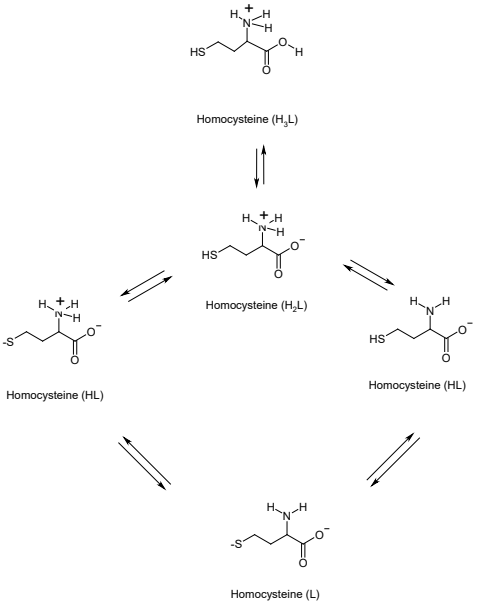

Fig.2: Schematic Representation Of Dissociation Of Homocysteine

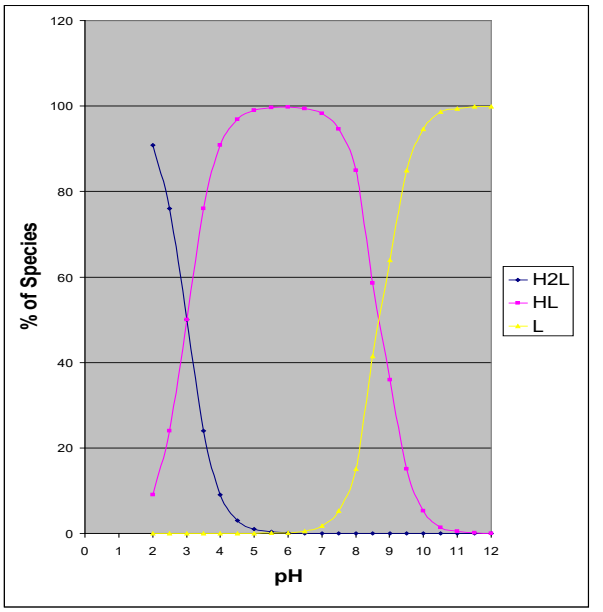

Fig.3: Ph-Species Distribution Profile For Free Homocysteine. Ordinate Represents The Percentage Of A Given Ligand Species As A Function Of The Total Concentration Tl = 0.002 Mol Dm-3 T = 37.00c ; M = 0.15 Mol Dm-3 (Kno3)

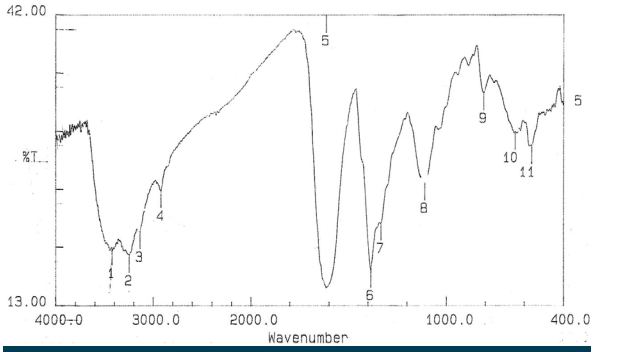

Fig.5: IR- Spectra of [Cu(hCy)(H2O)] Complex

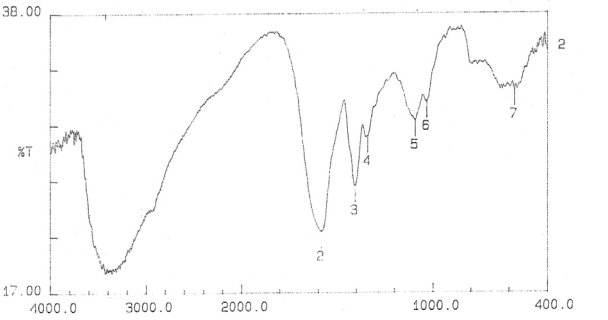

Fig.6: IR- Spectra of [Ni(hCy)(H2O)] Complex

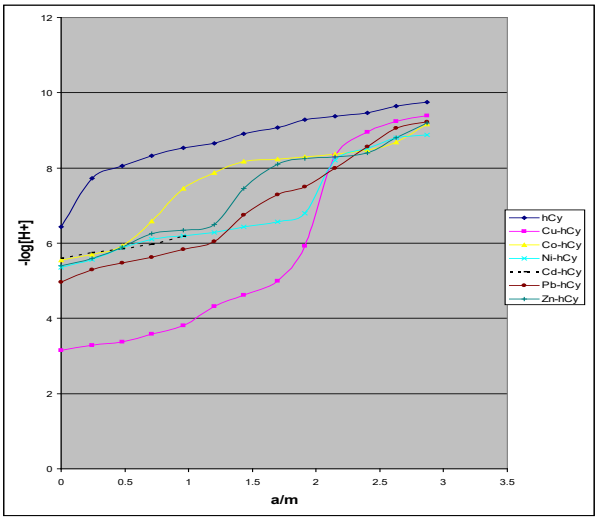

Fig.4: Potentiometric Titration Curves For Free Homocysteine And Metal {Cu (Ii), Ni (Ii), Pb (Ii) , Cd (Ii), And Co (Ii)} In A 1:1molar Ratio Tl = 0.0005 Mol Dm-3 ; Tm = 0.0005 Mol Dm-3 T = 37.00c ; M = 0.15 Mol Dm-3 (Kno3) A = Moles Of Base Added Per Mole Of The Ligand

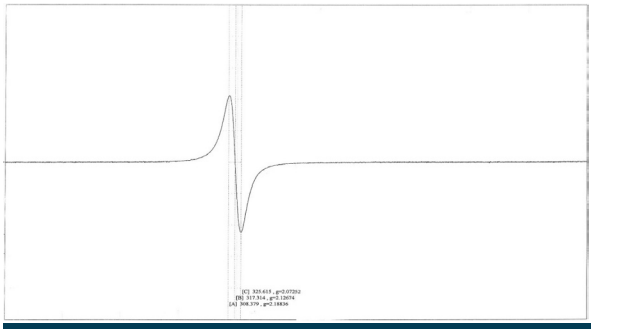

Fig.7: ESR Spectra of [Cu(hCy)(H2O)] complex

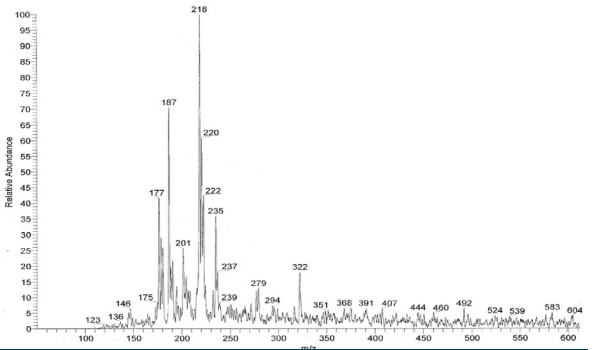

Fig.8: Mass Spectra Of [Cu(Hcy)(H2o)] Complex

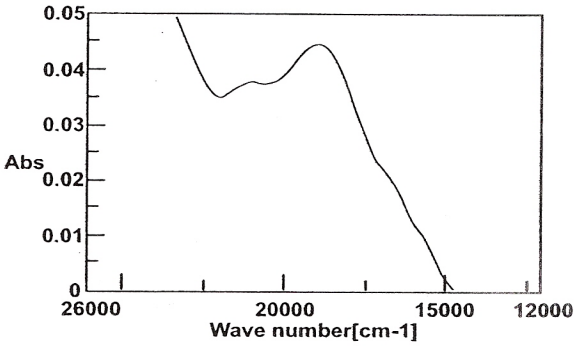

Fig.9: Electronic spectra of [Cu(hCy)(H2O)] complex

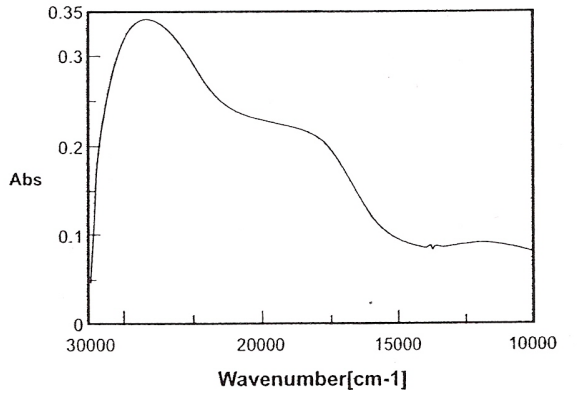

Fig.10: Electronic spectra of [Ni(hCy)(H2O)] complex

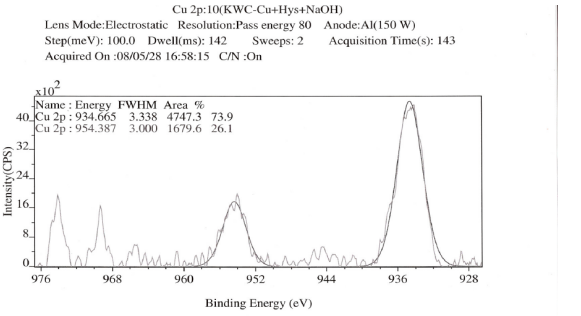

Fig.11a: Xps Spectra For [Cu(Hcy)(H2o)] Complex, B.e Values For Cu (2p) Atom In Copper Homocysteine Complex

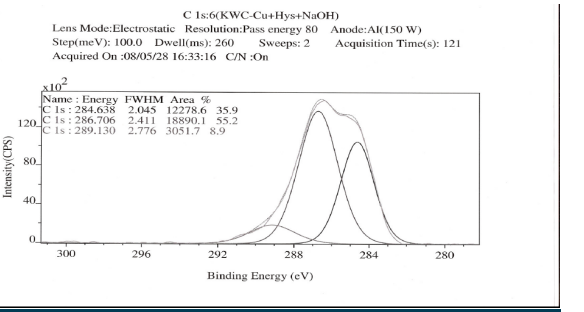

Fig.11b: XPS Spectra for [Cu(hCy)(H2O)] complex , B.E values for C (1s) atom in copper homocysteine complex

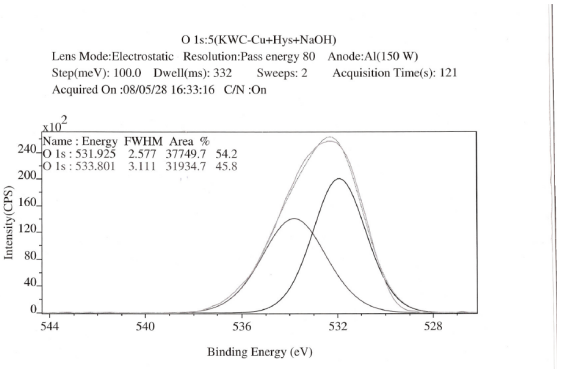

Fig.11c: XPS Spectra for[Cu(hCy)(H2O)] complex, B.E values for O (1s) atom in copper homocysteine

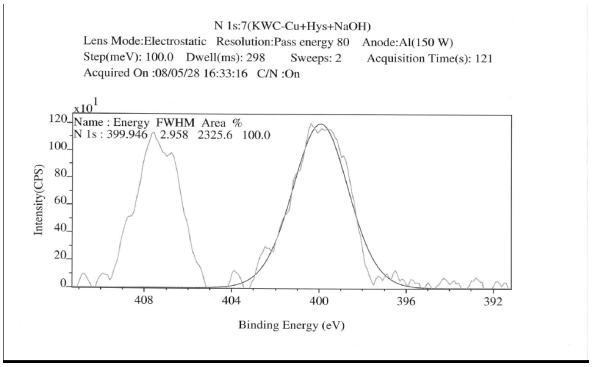

Fig.11d: XPS Spectra for [Cu(hCy)(H2O)] complex, B.E values for N (1s) atom in copper homocysteine complex

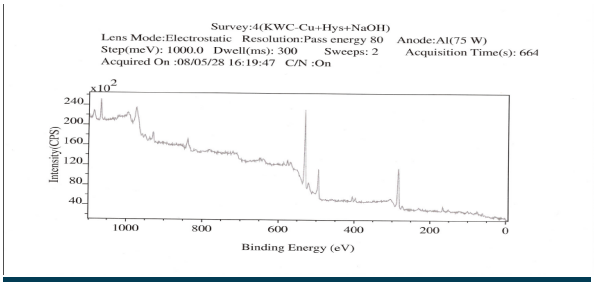

Fig.11e: XPS Spectra for [Cu(hCy)(H2O)] complex, Overall spectra of B.E values of Cu, C, O, N, & S atoms in copper homocysteine complex

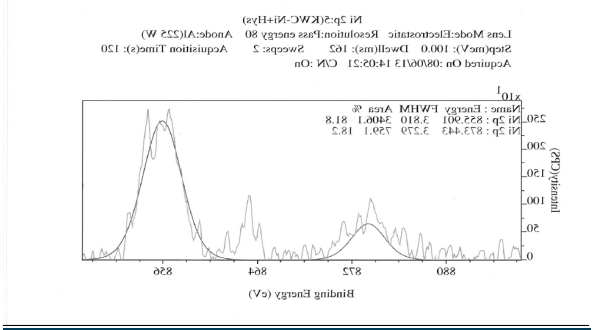

Fig.11f: XPS Spectra for [Cu(hCy)(H2O)] complex, Overall spectra of B.E values of Cu, C, O, N, & S atoms in copper homocysteine complex

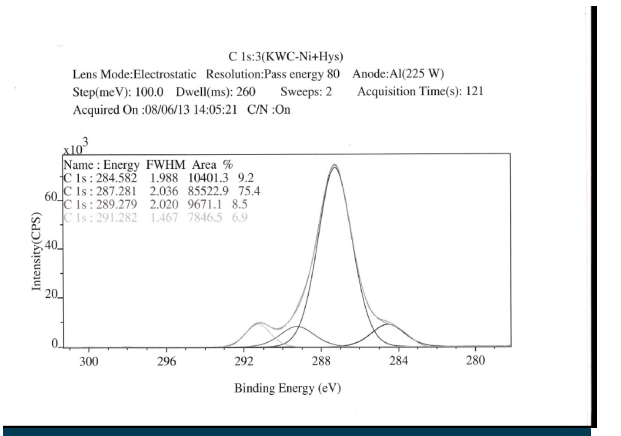

Fig.12a: B.E values for C (1s) atom in Nickel homocysteine complex

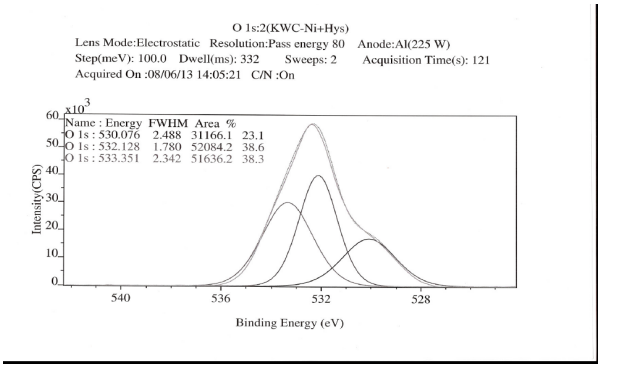

Fig.12b: XPS Spectra for [Ni(hCy)(H2O)] complex, B.E values for O (1s) atom in Nickel homocysteine complex

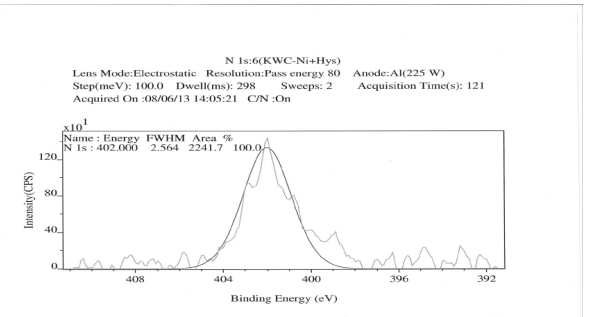

Fig.12c: XPS Spectra for [Ni(hCy)(H2O)] complex, B.E values for N (1s) atom in Nickel homocysteine complex

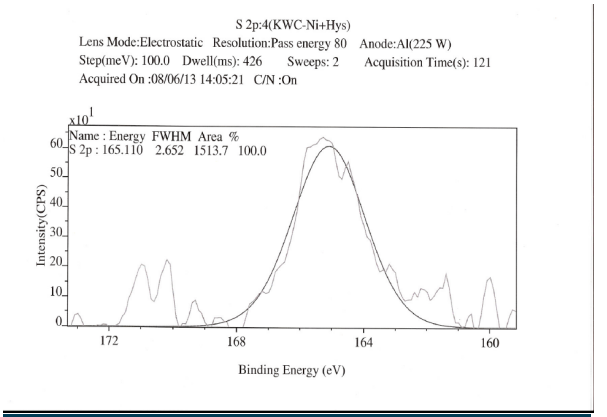

Fig.12d: XPS Spectra for [Ni(hCy)(H2O)] complex, B.E values for S (1s) atom in Nickel homocysteine complex

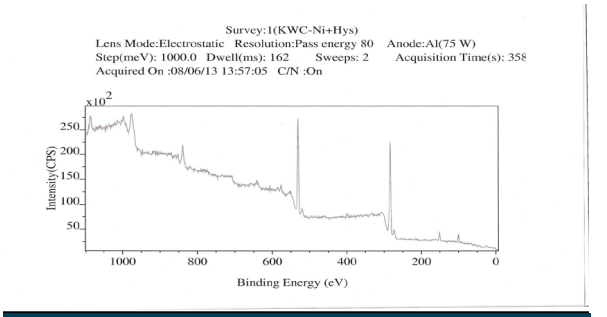

Fig.12e: Overall spectra of B.E values of Cu, C, O, N, & S atoms in Nickel homocysteine complex

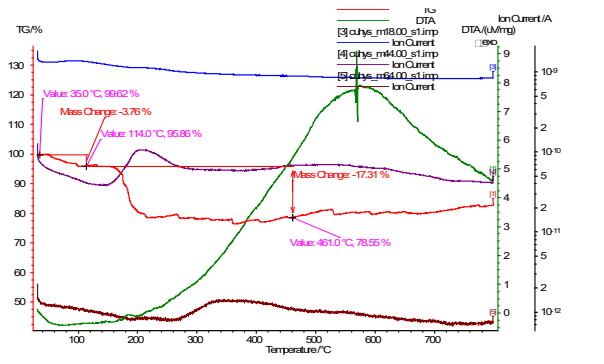

Fig.13: TGA diagram of (Cu(hCy)(H2O)

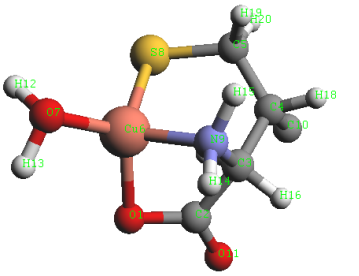

Fig.14: Molecular Modelling structure for copper complex (Cu(hCy)(H2O). The optimization of geometry and energy values were calculated by molecular mechanics software (System Type-Molecular Mechanical Hamiltonian UFF)

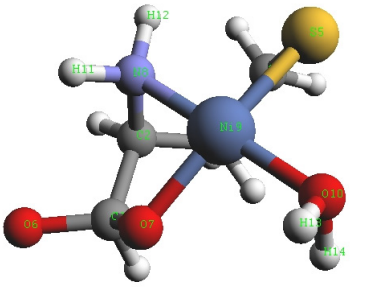

Fig.15: Molecular Modelling structure for nickel complex (Ni(hCy)(H2O). The optimization of geometry and energy values were calculated by molecular mechanics software (System Type-Molecular Mechanical Hamiltonian UFF)

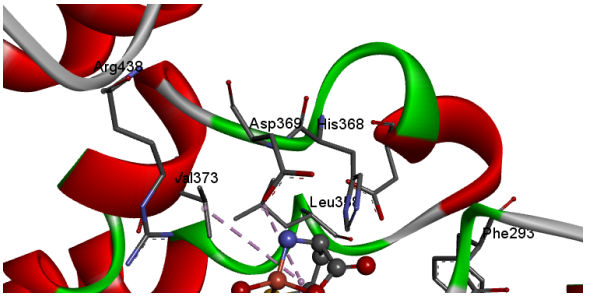

Fig.16a: The Copper homocysteine metal complex docked in the active site of Cytochrome C oxidase. Inhibitor molecule shown in stick style, amino acid side chains are shown in line style and protein shown in cartoon style.

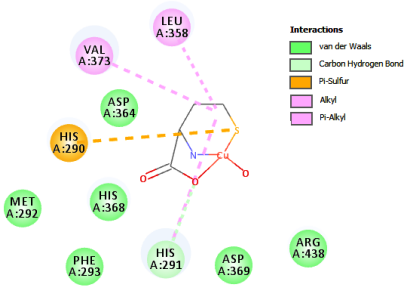

Fig.16b: The Copper homocysteine metal complex docked in the active site of Cytochrome C oxidase. The interactions between ligand and amino residues are shown here.

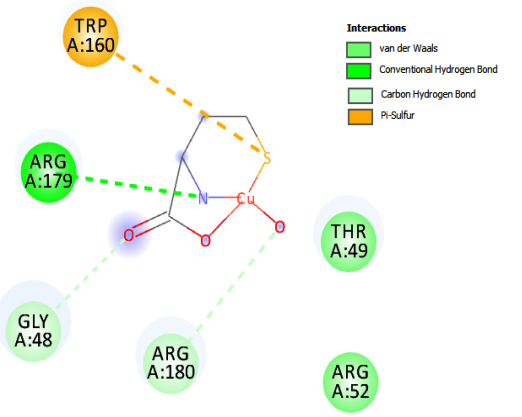

Fig.18b: The Copper homocysteine metal complex docked in the active site of Glutathione peroxidase 1. The interactions between ligand and amino residues are shown here.

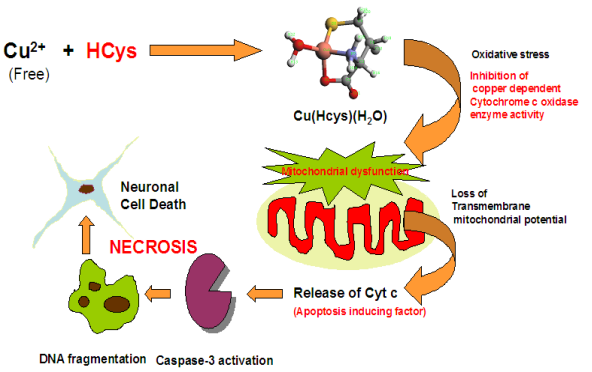

Fig.17: proposed mechanism for Copperhomocysteine complex toxicity

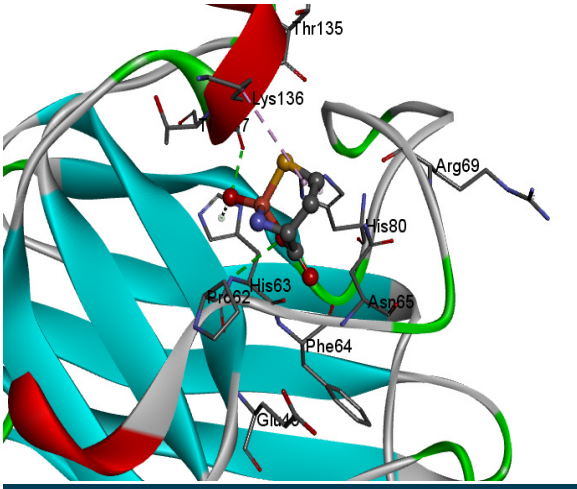

Fig.19a: The Copper homocysteine metal complex docked in the active site of Superoxide Dismutase 1. Inhibitor molecule shown in stick style, amino acid side chains are shown in line style and protein shown in cartoon style.

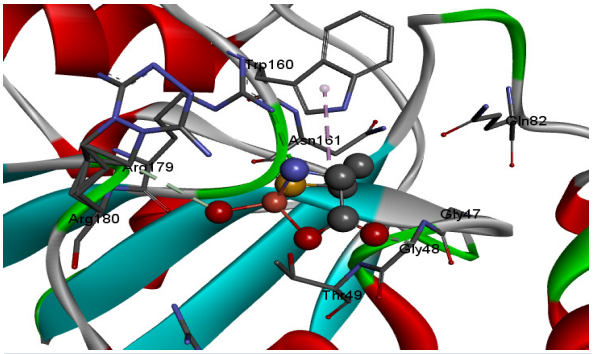

Fig.18a: The Copper homocysteine metal complex docked in the active site of Glutathione peroxidase 1. Inhibitor molecule shown in stick style, amino acid side chains are shown in line style and protein shown in cartoon style.

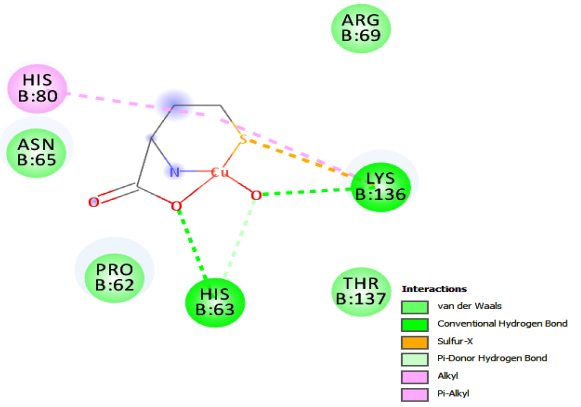

Fig.19b: The Copper homocysteine metal complex docked in the active site of Superoxide Dismutase 1. The interactions between ligand and amino residues are shown here.

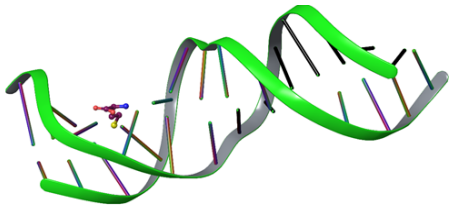

Binding mode of free homocysteine with DNA (Dock score=5.13)

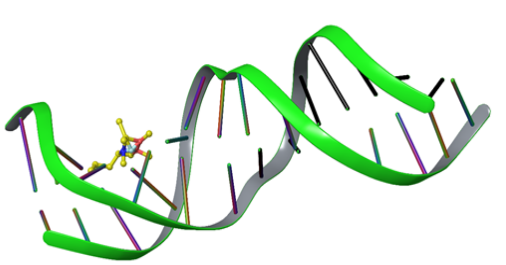

Binding mode of copper homocysteine complex with DNA (Dock score=6.13)

Fig.20a&b: Binding of Copperhomocysteine complex with DNA

REFERENCES

Ahmed, Mahmood & Qadir, Muhammad. 2014. Synthesis of Metal Complexes with Amino Acids for Animal Nutrition. Global Veterinaria. 12. 858-861.

Apostolova M.D., P. R Bontchev , B. B. Ivanova , W. R .Russell , D. R. Mehandjiev , J. H. Beattie, C. K., Nachev. 2003 .Copper-homocysteine complexes and potential physiological actions. J Inorg Biochem. Jul 1;95(4):321-33.
DOI: 10.1016/S0162-0134(03)00133-8
PMID: 12818803

Arunadevi, Alagarraj, and Natarajan Raman. 2020. "Biological response of Schiff base metal complexes incorporating amino acids-a short review." Journal of Coordination Chemistry 73.15 : 2095-2116.
DOI: 10.1080/00958972.2020.1824293

Bakavayev, S., N. Chetrit, T. Zvagelsky Mansour R.,Vyazmensky M., Barak Z., Israelson A., Engel S. 2019. Cu/Zn-superoxide dismutase and wild-type like fALS SOD1 mutants produce cytotoxic quantities of H2O2 via cysteine-dependent redox short-circuit. Sci Rep 9, 10826.
DOI: 10.1038/s41598-019-47326-x
PMID: 31346243 PMCID: PMC6658568

Bertini, I., H. B. Gray, E. L. Stiefel, J. S. Valentine, 2007 J.S. Biological Inorganic Chemistry. Structure and Reactivity; University Science Books: Mill Valley, CA, USA.

Bolotin S. N., E. L. Isaeva, M. H. Shamsutdinova, K. S. Pushkareva, and N. N. Bukov, 2009. Structure of Copper(II) Complexes with 2-[2-Hydroxy-Phenil]-4,4-Diphenyl-1,2-Dihydro4H-3,1-Benzoxazine in Chloroform, Advances in Physical Chemistry Volume , Article ID 365949.
DOI: 10.1155/2009/365949

Catalina Carrasco Pozo,, Alejandro a' lvarez-lueje, claudio olea-azar, camilo lo' pez-alarco' n, and herna' n speisky,2006. in vitro interaction between homocysteine and copper ions: potential redox implications, exp biol med 231:1569-1575.
DOI: 10.1177/153537020623100918
PMID: 17018882

Chandralekha S., G. Chandramohan. 2014. Synthesis, characterization and thermal analysis of the copper (II) complexes with 2,2'-bipyridyl and 1,10-phenanthroline , African Journal of Pure and Applied Chemistry, Vol. 8(10), pp. 162-175.
DOI: 10.5897/AJPAC2014.0592

Dayal S., G. L. Baumbach, E. Arning , T. Bottiglieri , F. M. Faraci , S. R. Lentz.2017. Deficiency of superoxide dismutase promotes cerebral vascular hypertrophy and vascular dysfunction in hyperhomocysteinemia. PLoS One. 2017 Apr 17;12(4):e0175732.
DOI: 10.1371/journal.pone.0175732
PMID: 28414812 PMCID: PMC5393600

Dong D., B. Wang , W. Yin , X. Ding , J. Yu , James Kang Y. 2013 Disturbance of Copper Homeostasis Is a Mechanism for Homocysteine-Induced Vascular Endothelial Cell Injury. PLoS ONE 8(10): e76209.
DOI: 10.1371/journal.pone.0076209
PMID: 24204604 PMCID: PMC3799909

Eichorn G. L., 1973. "Inorganic Biochemistry", Vols. 1 and 2, Ed., Elsevier, New York.

Fan, X., L. Zhang, H. Li, G. Chen, , G. Qi, X. Ma. and Y. Jin, 2020, Role of homocysteine in the development and progression of Parkinson's disease. Ann Clin Transl Neurol, 7: 2332-2338.
DOI: 10.1002/acn3.51227
PMID: 33085841 PMCID: PMC7664283

Farkas, E. & I. Sovago, 2007. Metal Complexes of Amino Acids and Peptides. ChemInform. 38.
DOI: 10.1002/chin.200742251

Ferré-D'., A.R. Amaré, W.C. Winkler 2011. The roles of metal ions in regulation by riboswitches. Met Ions Life Sci.;9:141-73.
DOI: 10.1039/9781849732512-00141
PMID: 22010271 PMCID: PMC3454353

Hughes M.N., 1981."Inorganic Chemistry of Biological processes", wiley,2 nd edition.,

Hultberg, Björn, Anders Andersson, and Anders Isaksson.1997 "The effects of homocysteine and copper ions on the concentration and redox status of thiols in cell line cultures." Clinica chimica acta 262.1-2 : 39-51.
DOI: 10.1016/S0009-8981(97)06531-5
PMID: 9204208

Ivanova B. B., M. G. Arnaudov, P. R. Bontchev, 2004.Linear-dichroic infrared spectral analysis of Cu(I)-homocysteine complex, Spectrochimica Acta Part A: Molecular and Biomolecular Spectroscopy, Volume 60, Issue 4, Pages 855-862.
DOI: 10.1016/S1386-1425(03)00310-X
PMID: 15036096

Kaluđerović G. N., S. Gómez-Ruiz, D. Maksimović-Ivanić, R. Paschke, S. Mijatović. 2012. Metals in medicine. Bioinorg Chem Appl.:705907.
DOI: 10.1155/2012/705907
PMID: 22956920 PMCID: PMC3432323

Katherine J. Franz and Nils Metzler-Nolte 2019 Chemical Reviews 119 (2), 727-729
DOI: 10.1021/acs.chemrev.8b00685
PMID: 30990707

Kazuo Nakamoto , 1978 Infrared and Raman Spectra of Inorganic and Coordination Compounds, Part B

Keskitalo, Salla & Farkas, Melinda & Hanenberg, Michael & Szodorai, Anita & Kulic, Luka & Semmler, Alexander & Weller, Michael & Nitsch, Roger & Linnebank, Michael. 2014. Reciprocal modulation of AÎ²42 aggregation by copper and homocysteine. Frontiers in aging neuroscience. 6. 237.
DOI: 10.3389/fnagi.2014.00237
PMID: 25249976 PMCID: PMC4157544

Ledda C, E. Cannizzaro, P. Lovreglio, E. Vitale, A. Stufano, A. Montana, G. Li Volti, V. Rapisarda. 2019. Exposure to Toxic Heavy Metals Can Influence Homocysteine Metabolism? Antioxidants (Basel). Dec 28;9(1):30.
DOI: 10.3390/antiox9010030
PMID: 31905706 PMCID: PMC7022705

Linnebank M., H. Lutz , E. Jarre , S. Vielhaber , C. Noelker , E. Struys , C. Jakobs , T. Klockgether, B. O. Evert, W. S. Kunz, U. Wüllner. 2006. Binding of copper is a mechanism of homocysteine toxicity leading to COX deficiency and apoptosis in primary neurons, PC12 and SHSY-5Y cells. Neurobiol Dis. Sep;23(3):725-30.
DOI: 10.1016/j.nbd.2006.06.010
PMID: 16876425

López-Gastélum, K.-A.; Velázquez-Contreras, E.F.; García, J.J.; Flores-Alamo, M.; Aguirre, G.; Chávez-Velasco, D.; Narayanan, J.; Rocha-Alonzo, F. Mononuclear and Tetranuclear Copper(II) Complexes Bearing Amino Acid Schiff Base Ligands: Structural Characterization and Catalytic Applications. Molecules 2021, *26*, 7301
DOI: 10.3390/molecules26237301
PMID: 34885882 PMCID: PMC8658810

Manjula, R., G. S. A. Wright, R. W. Strange and B. Padmanabhan. 2018, Assessment of ligand binding at a site relevant to SOD1 oxidation and aggregation. FEBS Lett, 592: 1725-1737.
DOI: 10.1002/1873-3468.13055
PMID: 29679384

Michael Linnebank, Holger Lutz, Eva Jarre, Stefan Vielhaber, Carmen Noelker, Eduard Struys, Cornelis Jakobs, Thomas Klockgether, Bernd O. Evert, Wolfram S. Kunz, Ullrich Wüllner, 2006, Binding of copper is a mechanism of homocysteine toxicity leading to COX deficiency and apoptosis in primary neurons, PC12 and SHSY-5Y cells,Neurobiology of Disease, Volume 23, Issue 3,725-730.
DOI: 10.1016/j.nbd.2006.06.010
PMID: 16876425

M.C. Mele., and Meucci E., (1996) *Amino Acids*, 11, 99-104
DOI: 10.1007/BF00805725
PMID: 24178642

Morris G. M, R. Huey, W, Lindstrom, M. F. Sanner,R. K. Belew, D. S. Goodsell, A. J. Olson. 2009. AutoDock4 and AutoDockTools4: Automated docking with selective receptor flexibility, J. Comput. Chem., 30, 2785-2791.
DOI: 10.1002/jcc.21256
PMID: 19399780 PMCID: PMC2760638

Ozturk Z., D. A. Kose, A. Asan et al.,2014. "Porous metal-organic Cu(II) complex of L-Arginine; 2synthesis, characterization, hydrogen storage properties and molecular simulation calculations," Hittite Journal of Science and Engineering, vol. 1, no. 1, pp. 1-5.
DOI: 10.17350/HJSE19030000001

Rajarajan, Govindasamy & Ezhumalai, Dhineshkumar & Amala, Syawaludin & M. Seenivasan, & A. Paramasivan. 2021. Determination of Stability constants Nickel binary and ternary complexes in aquesous DMSO by Pontentiometric method. Journal of Physics: Conference Series. 1724.
DOI: 10.1088/1742-6596/1724/1/012005

Roy Mason W., and B. Harry. 1968 Electronic Structures of Square-Planar Complexes Gray' Contribution No. 3664 from the Gates and Crellin Laboratories of Chemistry, California Institute of Technology, Pasadena, California 91 109.

Sayce IG. 1968.Computer calculation of equilibrium constants of species present in mixtures of metal ions and complexing agents. Talanta. Dec;15(12):1397-411.
DOI: 10.1016/0039-9140(68)80200-0
PMID: 18960446

Sigel H., Marcell Dekker, 1998. "Metal ions in Biological systems", Ed. Vols. 1 to 25, New York.

Smith, Robert M., J. Ramunas Motekaitis, and E. Arthur Martell. 1985 "Prediction of stability constants. II. Metal chelates of natural alkyl amino acids and their synthetic analogs." Inorganica chimica acta 103.1: 73-82.
DOI: 10.1016/S0020-1693(00)85215-9

Starkebaum, G., and Harlan, (1986) J. M. J. Clin. Ivest., 77, 1370-1376
DOI: 10.1172/JCI112442
PMID: 3514679 PMCID: PMC424498

Vijayalakshmi M, 2019 Synthesis and Characterization of Some Transition Metal Complexes of Schiff Base Derived From 2, 4 - Dihydroxybenzaldehyde; Iranian Journal of Pharmaceutical Sciences, 15 (3):29-40.

Xiao, Zuo & Dong, Daoyin & Sun, Miao & Xie, Huiqi & Kang, Y. James. 2013. Homocysteine Restricts Copper Availability Leading to Suppression of Cytochrome C Oxidase Activity in Phenylephrine-Treated Cardiomyocytes. PloS one. 8.
DOI: 10.1371/journal.pone.0067549
PMID: 23818984 PMCID: PMC3688604

Zong, S., M. Wu, J. Gu, Liu T., Guo R., Yang M. 2018. Structure of the intact 14-subunit human cytochrome c oxidase. Cell Res 28, 1026-1034.
DOI: 10.1038/s41422-018-0071-1
PMID: 30030519 PMCID: PMC6170408